Figure S1

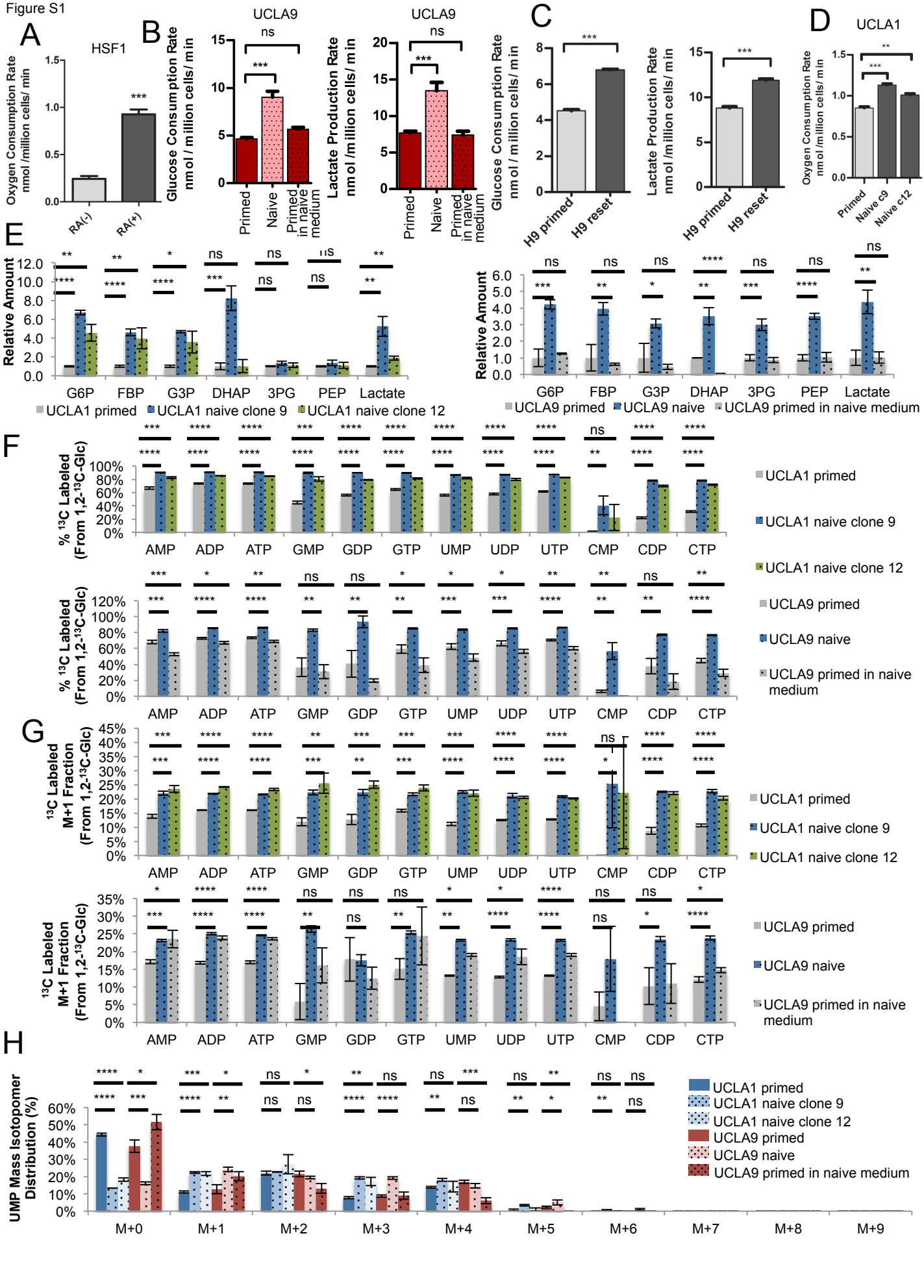
A
HSF1
Oxygen Consumption Rate nmol /million cells/ min
RA(-)
RA(+)
B
UCLA9
Glucose Consumption Rate nmol / million cells/ min
Lactate Production Rate nmol /million cells/ min
Primed
Naive
Primed in naive medium
C
Glucose Consumption Rate nmol / million cells/ min
Lactate Production Rate nmol /million cells/ min
H9 primed
H9 reset
D
UCLA1
Oxygen Consumption Rate nmol /million cells/ min
Primed
Naive c9
Naive c12
E
Relative Amount
G6P
FBP
G3P
DHAP
3PG
PEP
Lactate
UCLA1 primed
UCLA1 naive clone 9
UCLA1 naive clone 12
UCLA9 primed
UCLA9 naive
UCLA9 primed in naive medium
F
% 13C Labeled (From 1,2-13C-Glc)
AMP
ADP
ATP
GMP
GDP
GTP
UMP
UDP
UTP
CMP
CDP
CTP
G
13C Labeled M+1 Fraction (From 1,2-13C-Glc)
H
UMP Mass Isotopomer Distribution (%)
M+0
M+1
M+2
M+3
M+4
M+5
M+6
M+7
M+8
M+9

Figure S2

A

MENSSEN_MYC_TARGETS

URL: http://software.broadinstitute.org/gsea/msigdb/cards/MENSSEN_MYC_TARGETS

> Genes up-regulated by adenoviral expression of c-MYC [GeneID=4609] in HUVEC cells (umbilical vein endothelium).

APEX1	EIF5AL1	HSPD1	MSH2	RPS19
BRCA1	ENO1	HSPE1	NCL	RRP9
C1QBP	EPRS	HSPH1	NME1	RUVBL2
CCNB1	FKBP4	KAT2B	NOP56	SCARB1
CCT3	HERC5	KIAA0664	NPM1	SLPI
CDK4	HNRPDL	LDHA	NSF	SRM
DDX21	HSP90AA1	LDHB	NUTF2	TRAP1
DNAJB1	HSP90AB1	METAP2	PFKM	TSPO
EFTUD2	HSPA1A	MGST1	PHB	YWHAE
EI24	HSPA8	MNT	POLR2F	
EIF3B	HSPA9	MRPL3	PPIF	

B UCLA1 naive c9 versus primed hESCs

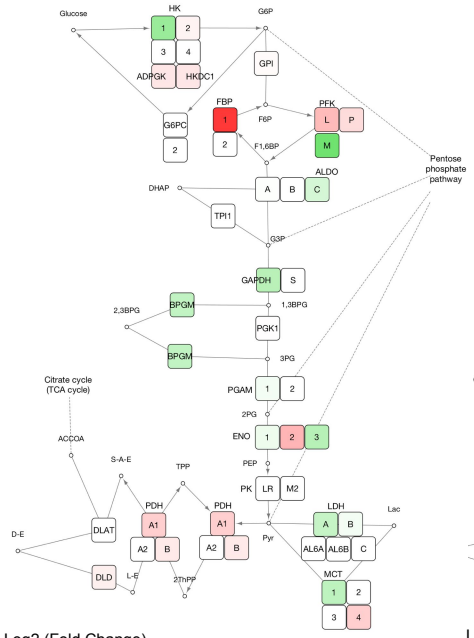

Log2 (Fold Change)

-4 4

Increased mRNA expression level in UCLA1 naive hESC clone 9

Increased mRNA expression level in UCLA1 primed hESCs

C UCLA1 naive c12 versus primed hESCs

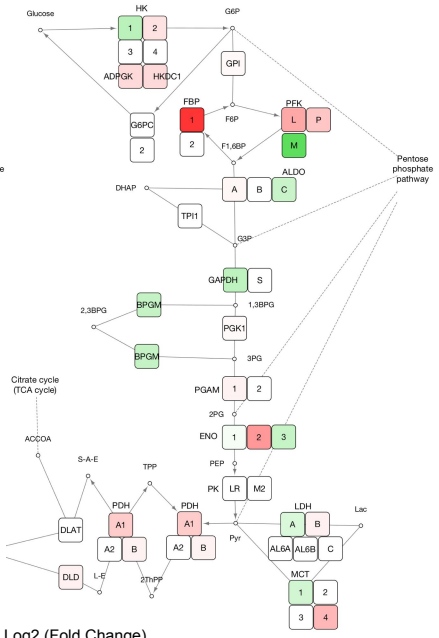

Log2 (Fold Change)

-4 4

Increased mRNA expression level in UCLA1 naive hESC clone 12

Increased mRNA expression level in UCLA1 primed hESCs

D Takashima et al. H9 reset versus primed hESCs

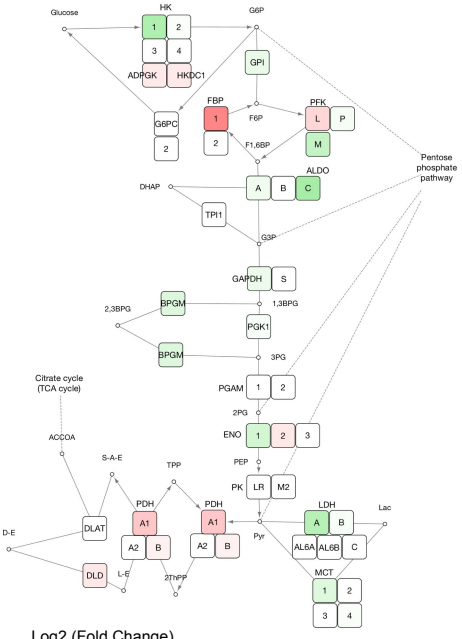

Log2 (Fold Change)

-4 4

Increased mRNA expression level in H9 reset hESCs by Takashima et al.

Increased mRNA expression level in H9 primed hESCs by Takashima et al.

E

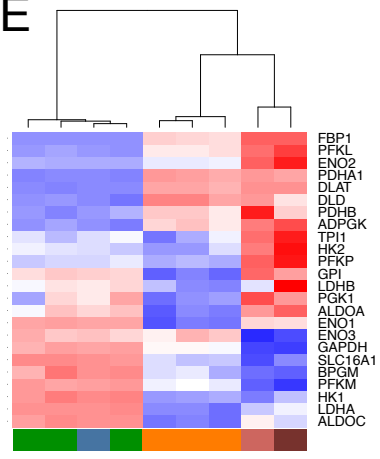

UCLA1 primed

UCLA1 naive clone 9

UCLA1 naive clone 12

H9 primed Takashima

H9 reset Takashima

Log2FC

-2 2

Z-Score

F

	Oocyte	2-cell	4-cell	6-cell	8 to 10-cell	Morula	Blastocyst	ESC
Oocyte vs	-	N.E.	0.77	N.E.	N.E.	N.E.	N.E.	N.E.
2-cell vs	0.89	-	1.52	N.E.	N.E.	N.E.	N.E.	N.E.
4-cell vs	N.E.	N.E.	-	N.E.	N.E.	N.E.	N.E.	N.E.
6-cell vs	1.33	1.07	1.72	-	N.E.	N.E.	N.E.	N.E.
8 to 10-cell vs	2.64	2.59	2.24	2.47	-	N.E.	N.E.	1.2
Morula vs	1.92	1.91	2.44	2.51	0.97	-	1.11	1.78
Blastocyst vs	2.29	2.01	2.13	2.58	0.98	N.E.	-	1.57
ESC vs	2.22	2.32	2.23	2.15	N.E.	N.E.	N.E.	-

N.E. = Not enriched

Normalized enrichment score

0.5 4.0

G

Enrichment plot: MENSSEN_MYC_TARGETS

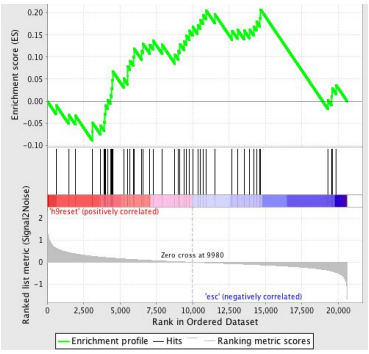

H9 reset versus primed hESCs
Microarray data by Takashima et al.
ES = 0.207, NES = 1.69
p = 0.030, FDR = 0.080

Figure S3

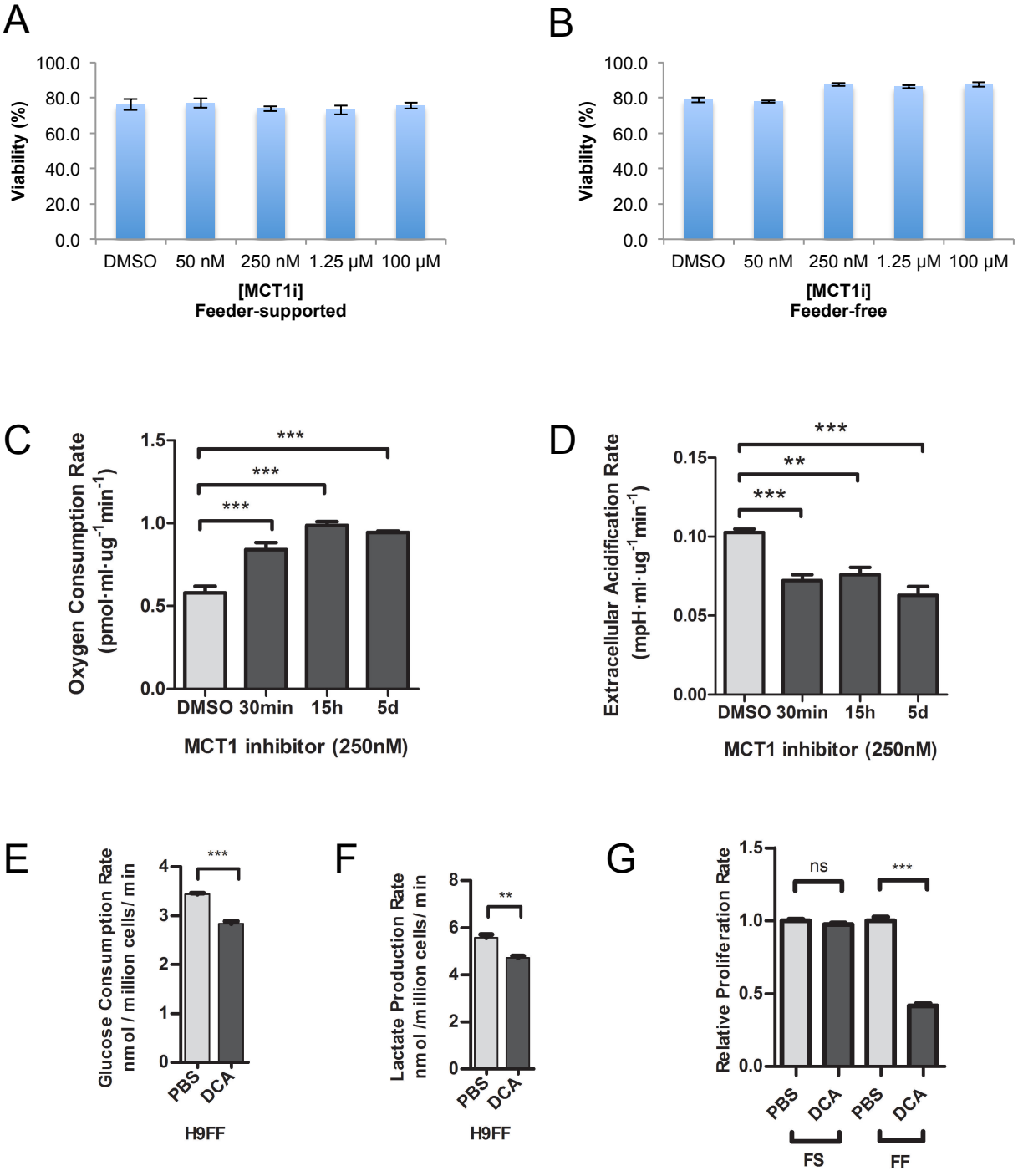
A
Viability (%)
100.0
80.0
60.0
40.0
20.0
0.0
DMSO
50 nM
250 nM
1.25 µM
100 µM
[MCT1i]
Feeder-supported
B
Viability (%)
100.0
80.0
60.0
40.0
20.0
0.0
DMSO
50 nM
250 nM
1.25 µM
100 µM
[MCT1i]
Feeder-free
C
Oxygen Consumption Rate
(pmol·ml·ug-1min-1)
1.5
1.0
0.5
0.0
***
***
***
DMSO
30min
15h
5d
MCT1 inhibitor (250nM)
D
Extracellular Acidification Rate
(mpH·ml·ug-1min-1)
0.15
0.10
0.05
0.00
***
**
***
DMSO
30min
15h
5d
MCT1 inhibitor (250nM)
E
Glucose Consumption Rate
nmol / million cells/ min
4
3
2
1
0
***
PBS
DCA
H9FF
F
Lactate Production Rate
nmol /million cells/ min
8
6
4
2
0
**
PBS
DCA
H9FF
G
Relative Proliferation Rate
1.5
1.0
0.5
0.0
ns
***
PBS
DCA
PBS
DCA
FS
FF

Figure S4

A

$$\text{Percent labeled} = \frac{\text{Labeled signal}}{\text{Labeled signal + Unlabeled signal}} = \frac{M_{+1} + M_{+2} + M_{+3} + \ldots + M_{+N}}{M_0 + M_{+1} + M_{+2} + M_{+3} + \ldots + M_{+N}}$$

where M_0 is the amount of the monoisotopic compound, M_{+1} is the amount of the compound with one ^{13}C atom, M_{+2} is the amount of the compound with 2 x ^{13}C atoms and so on; N is the number of carbon atoms in the molecule. (Yuan et al., 2008; Fan et al., 2014)

Percent labeled after correction =

$$\frac{(\text{Labeled signal})_{\text{FS hESCs}} - (\text{Labeled signal})_{\text{MEFs}}}{[(\text{Labeled signal})_{\text{FS hESCs}} - (\text{Labeled signal})_{\text{MEFs}}] + [(\text{Unlabeled signal})_{\text{FS hESCs}} - (\text{Unlabeled signal})_{\text{MEFs}}]}$$

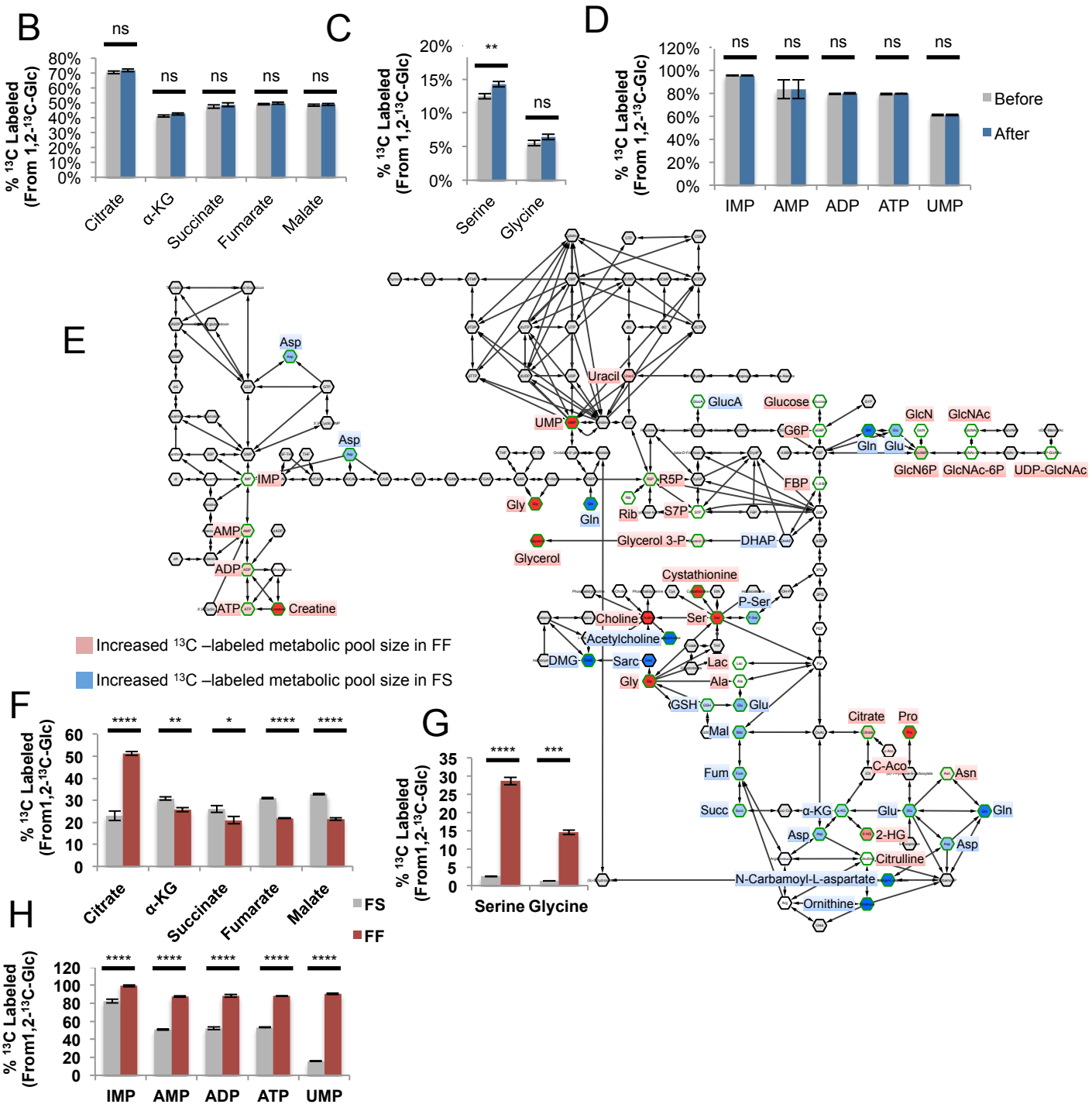

Figure S5

A

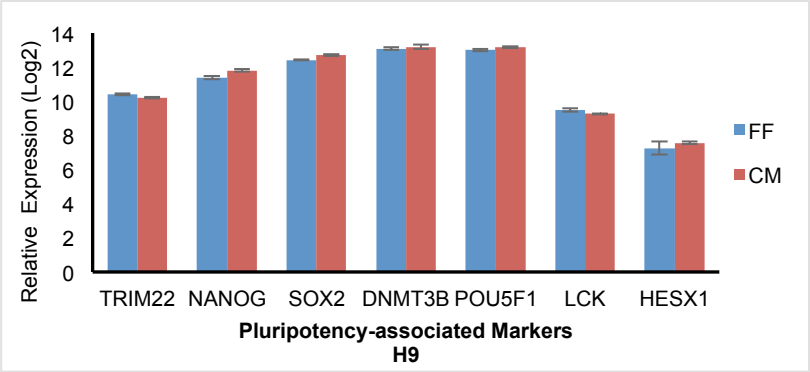
Relative Expression (Log2)
14
12
10
8
6
4
2
0
TRIM22
NANOG
SOX2
DNMT3B
POU5F1
LCK
HESX1
FF
CM
Pluripotency-associated Markers
H9

B

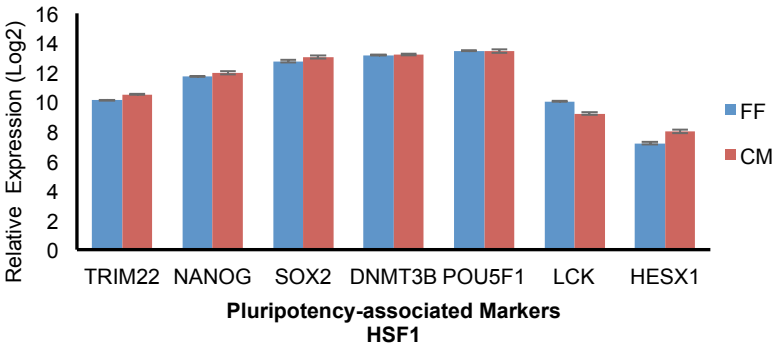
Relative Expression (Log2)
16
14
12
10
8
6
4
2
0
TRIM22
NANOG
SOX2
DNMT3B
POU5F1
LCK
HESX1
FF
CM
Pluripotency-associated Markers
HSF1

Figure S6

A

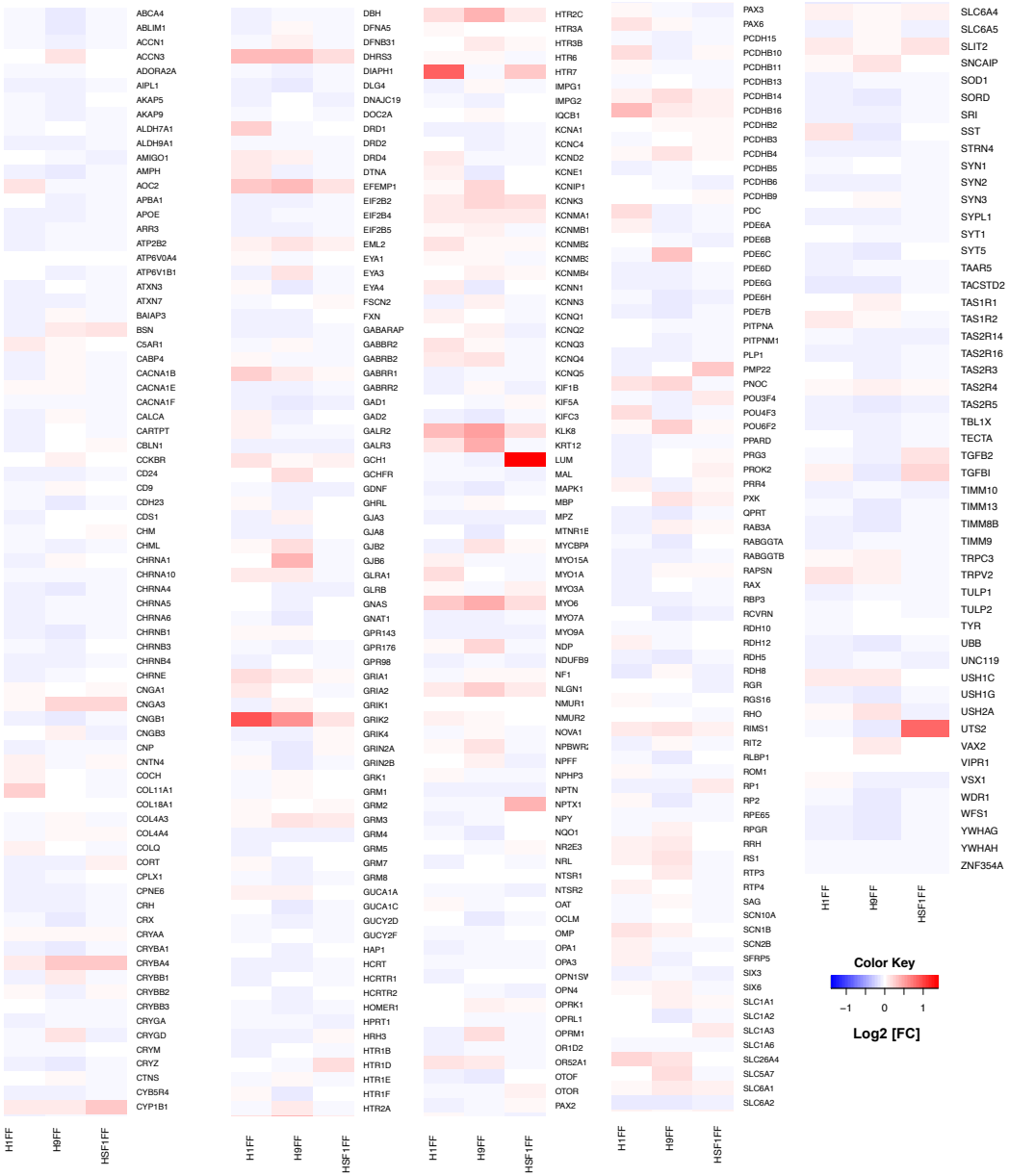
ABCA4
ABLIM1
ACCN1
ACCN3
ADORA2A
AIPL1
AKAP5
AKAP9
ALDH7A1
ALDH9A1
AMIGO1
AMPH
AOC2
APBA1
APOE
ARR3
ATP2B2
ATP6V0A4
ATP6V1B1
ATXN3
ATXN7
BAIAP3
BSN
C5AR1
CABP4
CACNA1B
CACNA1E
CACNA1F
CALCA
CARTPT
CBLN1
CCKBR
CD24
CD9
CDH23
CDS1
CHM
CHML
CHRNA1
CHRNA10
CHRNA4
CHRNA5
CHRNA6
CHRNB1
CHRNB3
CHRNB4
CHRNE
CNGA1
CNGA3
CNGB1
CNGB3
CNP
CNTN4
COCH
COL11A1
COL18A1
COL4A3
COL4A4
COLQ
CORT
CPLX1
CPNE6
CRH
CRX
CRYAA
CRYBA1
CRYBA4
CRYBB1
CRYBB2
CRYBB3
CRYGA
CRYGD
CRYM
CRYZ
CTNS
CYB5R4
CYP1B1
DBH
DFNA5
DFNB31
DHRS3
DIAPH1
DLG4
DNAJC19
DOC2A
DRD1
DRD2
DRD4
DTNA
EFEMP1
EIF2B2
EIF2B4
EIF2B5
EML2
EYA1
EYA3
EYA4
FSCN2
FXN
GABARAP
GABBR2
GABRB2
GABRR1
GABRR2
GAD1
GAD2
GALR2
GALR3
GCH1
GCHFR
GDNF
GHRL
GJA3
GJA8
GJB2
GJB6
GLRA1
GLRB
GNAS
GNAT1
GPR143
GPR176
GPR98
GRIA1
GRIA2
GRIK1
GRIK2
GRIK4
GRIN2A
GRIN2B
GRK1
GRM1
GRM2
GRM3
GRM4
GRM5
GRM7
GRM8
GUCA1A
GUCA1C
GUCY2D
GUCY2F
HAP1
HCRT
HCRTR1
HCRTR2
HOMER1
HPRT1
HRH3
HTR1B
HTR1D
HTR1E
HTR1F
HTR2A
HTR2C
HTR3A
HTR3B
HTR6
HTR7
IMPG1
IMPG2
IQCB1
KCNA1
KCNC4
KCND2
KCNE1
KCNIP1
KCNK3
KCNMA1
KCNMB1
KCNMB2
KCNMB3
KCNMB4
KCNN1
KCNN3
KCNQ1
KCNQ2
KCNQ3
KCNQ4
KCNQ5
KIF1B
KIF5A
KIFC3
KLK8
KRT12
LUM
MAL
MAPK1
MBP
MPZ
MTNR1B
MYCBPAP
MYO15A
MYO1A
MYO3A
MYO6
MYO7A
MYO9A
NDP
NDUFB9
NF1
NLGN1
NMUR1
NMUR2
NOVA1
NPBWR2
NPFF
NPHP3
NPTN
NPTX1
NPY
NQO1
NR2E3
NRL
NTSR1
NTSR2
OAT
OCLM
OMP
OPA1
OPA3
OPN1SW
OPN4
OPRK1
OPRL1
OPRM1
OR1D2
OR52A1
OTOF
OTOR
PAX2
PAX3
PAX6
PCDH15
PCDHB10
PCDHB11
PCDHB13
PCDHB14
PCDHB16
PCDHB2
PCDHB3
PCDHB4
PCDHB5
PCDHB6
PCDHB9
PDC
PDE6A
PDE6B
PDE6C
PDE6D
PDE6G
PDE6H
PDE7B
PITPNA
PITPNM1
PLP1
PMP22
PNOC
POU3F4
POU4F3
POU6F2
PPARD
PRG3
PROK2
PRR4
PXK
QPRT
RAB3A
RABGGTA
RABGGTB
RAPSN
RAX
RBP3
RCVRN
RDH10
RDH12
RDH5
RDH8
RGR
RGS16
RHO
RIMS1
RIT2
RLBP1
ROM1
RP1
RP2
RPE65
RPGR
RRH
RS1
RTP3
RTP4
SAG
SCN10A
SCN1B
SCN2B
SFRP5
SIX3
SIX6
SLC1A1
SLC1A2
SLC1A3
SLC1A6
SLC26A4
SLC5A7
SLC6A1
SLC6A2
SLC6A4
SLC6A5
SLIT2
SNCAIP
SOD1
SORD
SRI
SST
STRN4
SYN1
SYN2
SYN3
SYPL1
SYT1
SYT5
TAAR5
TACSTD2
TAS1R1
TAS1R2
TAS2R14
TAS2R16
TAS2R3
TAS2R4
TAS2R5
TBL1X
TECTA
TGFB2
TGFBI
TIMM10
TIMM13
TIMM8B
TIMM9
TRPC3
TRPV2
TULP1
TULP2
TYR
UBB
UNC119
USH1C
USH1G
USH2A
UTS2
VAX2
VIPR1
VSX1
WDR1
WFS1
YWHAG
YWHAH
ZNF354A
H1FF
H9FF
HSF1FF
Color Key
−1
0
1
Log2 [FC]

B

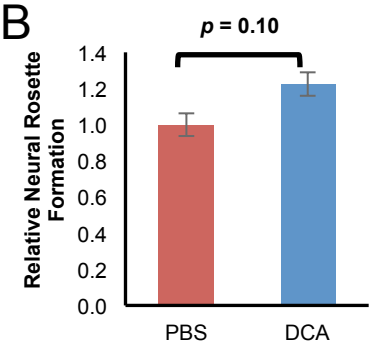
p = 0.10
Relative Neural Rosette Formation
1.4
1.2
1.0
0.8
0.6
0.4
0.2
0.0
PBS
DCA

Figure S7

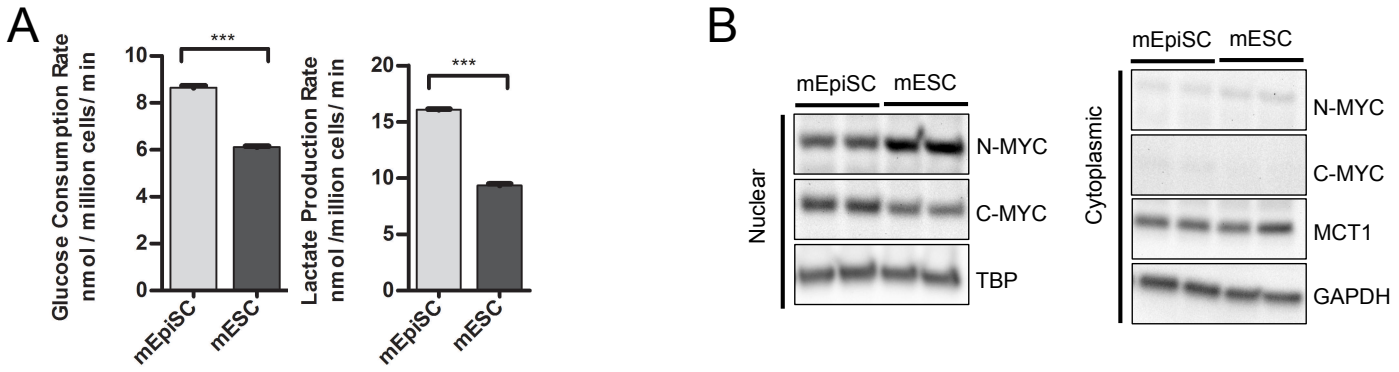
A
Glucose Consumption Rate
nmol / million cells/ min
10
8
6
4
2
0
***
mEpiSC
mESC
Lactate Production Rate
nmol /million cells/ min
20
15
10
5
0
***
mEpiSC
mESC
B
mEpiSC
mESC
Nuclear
N-MYC
C-MYC
TBP
mEpiSC
mESC
Cytoplasmic
N-MYC
C-MYC
MCT1
GAPDH

SUPPLEMENTAL FIGURE AND TABLE LEGENDS

Figure S1. Related to Figure 1. Naive hESCs exhibit increased glycolysis. (A) Oxygen consumption rates in FS HSF1 hESCs, treated for 7 days with DMSO (RA (-)) or 10 μM retinoic acid (RA (+)), as measured by an anaerobic chamber fitted with a fiber optic oxygen sensor. (B) Glucose consumption and lactate production rates of primed UCLA9 hESCs, naive UCLA9 hESCs generated by the 5i/LAF method, and primed UCLA9 hESCs placed in naive cell medium for 24 hours. (C) Glucose consumption rates (left) and lactate production rates (right) of primed H9 hESCs and naive/reset H9 hESCs generated by the Takashima et al. method (Takashima et al., 2014). (D) Oxygen consumption rates of primed UCLA1 hESCs and naive UCLA1 hESC clone 9 and clone 12 generated by the 5i/LAF method. For (E) – (H), primed UCLA1 hESCs, naive UCLA1 hESC clone 9 and clone 12, and primed UCLA9 hESCs, naive UCLA9 hESC, and primed UCLA9 hESCs placed in naive cell medium, were cultured in medium containing 1,2-^{13}C-glucose for 24 hours prior to metabolite extraction and analysis by LC-MS. (E) Relative amounts of indicated glycolytic intermediates extracted from the indicated cells. (F) Percentages of the indicated ^{13}C-labeled nucleotides extracted from the indicated cells. (G) Percentages of the indicated ^{13}C-labeled M+1 form of nucleotides extracted from the indicated cells. (H) Mass isotopomer distribution of the indicated ^{13}C-labeled UMP extracted from the indicated cells. For (A) - (H), error bars indicate ± 1 SEM of biological replicates (n = 3). ns: not significant; * $p < 0.05$; ** $p < 0.01$; *** $p < 0.001$; **** $p < 0.0001$.

Figure S2. Related to Figure 2. Glycolysis pathway gene expression changes upon the acquisition of naive pluripotency. (A) Members of the MYC target gene set by Menssen et al. Cytoscape network map showing the fold change of KEGG glycolysis genes in naive UCLA1 hESC clone 9 versus primed UCLA1 hESCs (B), naive UCLA1 hESC clone 12 versus primed UCLA1 hESCs (C), and Takashima reset versus primed H9 hESCs (D). Genes in red indicate increased mRNA expression levels in naive or reset cells. Genes in green indicate increased mRNA expression levels in primed cells. (E) Heatmap depicting log2 fold changes of KEGG glycolysis genes across UCLA1 primed, UCLA1 naive clone 9 and clone 12, and Takashima reset and primed H9 hESCs. Bottom colored bars indicate sample origins. (F) Heatmap showing the enrichment of MYC-regulated genes across various early human embryo development stages from Vassena et al. dataset. Each cell contains the normalized enrichment score (NES), based on GSEA, from pairwise comparison of two different cell types, as indicated. N.E.: not enriched. (G) GSEA mountain plot displaying enrichment of MYC-regulated genes in H9 reset versus primed hESCs.

Figure S3. Related to Figure 3. Manipulation of hESC metabolism via MCT1 inhibition. Cell viabilities of feeder-supported (A) and feeder-free (B) primed H9 hESCs treated with DMSO or AZD3965 at indicated concentrations for 24 hours, as determined by Trypan Blue staining. Oxygen consumption rates (C) and extracellular acidification rates (D) in FF H9 hESCs, treated with DMSO or 250 nM AZD3965 for the indicated times, as measured by XF24 Extracellular Flux Analyzer. Glucose consumption rates (E) and lactate production rates (F) of FF primed H9 hESCs treated with PBS or 5 mM

dichloroacetic acid (DCA) for 24 hours. (G) Proliferation rates of feeder-supported (FS) versus feeder-free (FF) H9 hESCs treated with PBS or 5 mM dichloroacetic acid (DCA) for 5 days. For (A) – (G), error bars indicate ± 1 SEM of biological replicates (n = 3). ns: not significant; ** $p < 0.01$, *** $p < 0.001$.

Figure S4. Related to Figure 4. Feeder-free Cultured hESCs Exhibit Increased Anabolic Glucose Metabolism Relative to Feeder Supported hESCs. (A) The formulas applied to calculate the effect of MEFs on the ^{13}C glucose labeling pattern of feeder supported hESCs. (B) Incorporation of ^{13}C labeled glucose into TCA cycle metabolites, and (C) serine and glycine, and (D) nucleotides in feeder supported UCLA1 hESCs before and after the mathematical correction. Feeder supported UCLA1 hESCs and MEFs alone were cultured in medium with 1,2-^{13}C-glucose for 24 hours. Extracted metabolites were analyzed by LC-MS, and the percentage of ^{13}C-labeled metabolites was compared. (E) Cytoscape network map showing differential use of glucose in many metabolic pathways in FS versus FF H1 hESCs. Metabolites in red indicate increased incorporation of 1,2-^{13}C-glucose carbons in FF hESCs compared to FS hESCs. Metabolites in blue indicate increased incorporation of 1,2-^{13}C-glucose carbons in FS hESCs compared to FF hESCs. Green borders indicate where the changes in incorporation of 1,2-^{13}C-glucose in FS hESCs compared to FF hESCs are statistically significant ($p < 0.05$). Metabolites in white indicate similar incorporation of 1,2-^{13}C-glucose carbons in FS hESCs compared to FF hESCs. Metabolites in grey are undetected. (F) Percentages of the indicated ^{13}C-labeled TCA cycle metabolites in FS versus FF H1 hESCs. (G) Percentages of ^{13}C-labeled serine and glycine in FS versus FF H1 hESCs.

(H) Percentages of ^{13}C-labeled nucleotides in FS versus FF H1 hESCs. For (B) – (D) and (F) – (H), error bars indicate ± 1 SEM of biological replicates (n = 3). ns: not significant; * $p < 0.05$; ** $p < 0.01$; *** $p < 0.001$; **** $p < 0.0001$.

Figure S5. Related to Figure 5. MEF-conditioned medium treatment does not change pluripotency-associated transcripts in primed feeder-free hESCs. mRNA levels of TRIM22, NANOG, SOX2, DNMT3B, POU5F1, LCK, and HESX1 in feeder-free (FF) versus MEF-conditioned medium treated FF (CM) H9 (A) and HSF1 (B) primed hESCs. Error bars indicate ± 1 SD of biological replicates (n=3).

Figure S6. Related to Figure 7. MCT1 inhibition of feeder free-cultured primed hESCs promotes neural lineage specification. (A) Heatmap representation of the relative fold changes (base 2) of the genes from the gene ontology term "neurological system process" after five days AZD3965 versus DMSO treatment of primed feeder-free H9, H1, and HSF1 hESCs. (B) Neural rosette formation efficiency of primed feeder-free hESCs treated with rosette formation media supplemented with PBS or 5 mM dichloroacetic acid (DCA) for 10 days. The number of rosette structures was quantified. Error bars indicate ± 1 SEM of biological replicates (n = 3).

Figure S7. Mouse embryonic stem cells exhibit lower glycolytic rates compared to mouse epiblast stem cells. (A) Glucose consumption rates (left) and lactate production rates (right) of mEpiSCs derived from in vivo epiblast and mESCs cultured in 2i/LIF condition. Error bars indicate ± 1 SEM of biological replicates (n = 3). *** $p < 0.001$.

(B) Immunoblot showing nuclear and cytoplasmic N-MYC and C-MYC levels in mEpiSCs derived from *in vivo* epiblast and mESCs cultured in 2i/LIF condition. Cytoplasmic MCT1 levels are also shown. TBP is used a loading control for the nuclear lysates. GAPDH is used as a loading control for the cytoplasmic lysates. Lysates were prepared in biological duplicates.

Table S1. Related to Figure 7. Input list of ranked genes for GO analysis by GOrilla.

SUPPLEMENTAL EXPERIMENTAL PROCEDURES

Cell Culture

Conventional feeder-supported human ESC lines H1, H9 (WiCell Research Institute, Inc., Madison, WI), HSF1 (University of California San Francisco, San Francisco, CA), UCLA1, and UCLA9 (University of California Los Angeles, Los Angeles, CA) were maintained on radiation inactivated MEF feeder layers (GlobalStem) and passed enzymatically by treatment for 2 min with 1 mg/ml Collagenase type IV (STEMCELL Technologies), and then mechanically lifted by using a cell scraper (Falcon), followed by passing through a 100-μm cell strainer. Conventional feeder-supported human ESCs were cultured in human ESC medium (hESM) – DMEM/F12 (Invitrogen) supplemented with 20% KSR (Invitrogen), 1% nonessential amino acids (NEAA, Invitrogen), 0.1 mM β-mercaptoethanol (Invitrogen), and 10 ng/ml FGF2 (Peprotech). Primed feeder-free human ESC lines H1, H9, and HSF1 were cultured on plates pre-coated with 1:25 diluted Matrigel (BD Biosciences) in mTeSR1 medium (STEMCELL Technologies). Tissue culture media were filtered using a low protein-binding 0.22 μm filter (Millipore). All experiments were performed under 5% CO_2 and atmospheric oxygen levels.

Naive human pluripotent stem cells were generated and maintained using the 5i/LAF condition exactly as described (Theunissen et al., 2014). Briefly, feeder-supported UCLA1 and UCLA9 hESCs were grown to ~ 60% density and fed hESM supplemented with 10 μM ROCK inhibitor Y-27632 (Stemgent). The following day, hESCs were trypsinized to single cell (0.05% Trypsin, ThermoFisher Scientific) and plated on feeders at 2 x 10^5 cells/well of a 6-well dish in hESM with ROCKi. Two days later culture medium was switched to 5i/LAF (1 μM PD0325901, 10 μM Y-27632 (Stemgent), 1 μM

IM-12 (Enzo), 0.5 μM SB590885 (R&D), 1 μM WH-4-023 (A Chemtek), 20 ng/ml recombinant hLIF (Millipore), 20 ng/ml Activin A (Peprotech), and 8 ng/ml FGF2 (R&D) in a 1:1 mixture of DMEM/F12 and Neurobasal medium (Invitrogen) supplemented with 1x N2, B27, NEAA, Pen/Strep, Glutamine (Invitrogen), 0.1 mM beta-mercaptoethanol, 0.5% KSR and 50 μg/ml BSA). Medium was changed daily, and in 8-10 days, after massive cell death, several dome-shaped colonies appeared. These colonies were passaged using Accutase (ThermoFisher Scientific). After 3-4 passages naive hESCs had expanded enough to be split at 1:4 or 1:5 ratio every 5 days. Before plating cells were passed through 40-μm mesh since naive hESCs grow best when plated as single cells. Feeder-supported naive line UCLA19 was derived directly from the inner cell mass of a human blastocyst and since cultured in 5i/LAF medium.

Another naive human pluripotent stem cell line, H9 reset, was maintained using the Takashima et al. method exactly as described (Takashima et al., 2014), and cultured in an incubator with 5% O_2 and 5% CO_2 at 37 °C. For comparing the glycolytic rates in reset versus primed H9 hESCs, both reset and primed cells were received from the Austin Smith Lab and cultured under 5% O_2 condition.

Neural rosette differentiation was induced by treatment with DMEM/F12 supplemented with B27 and N2 (Gibco), 1 μM retinoic acid (Sigma), 20 ng/ml FGF2, and 1 μM purmorphamine (Cayman chemical) for 10 days.

Cells were treated with AZD3965 (AstraZeneca, 250 nM) or CD532 (Millipore, 25 – 250 nM) for indicated times to assess the effects of MCT1 inhibition or N-MYC inhibition.

Immunostaining of Human Preimplantation Embryos

All experiments were performed using human embryos that were excess to infertility treatment and donated for research following informed consent in accordance with the guidelines established by UCLA Embryonic Stem Cell Research Oversight (ESCRO) Committee and the Committee on the Use of Human Subjects Institutional Review Board (IRB).

Human blastocysts were thawed using Vit Kit-Thaw (Irvine Scientific) according to manufacturer protocol. The embryos were cultured in drops of Continuous Single Culture medium (Irvine Scientific) supplemented with 20% Quinn's Advantage SPS Serum Protein Substitute (Sage Media) under mineral oil (Irvine Scientific) overnight at 37 °C, 6% CO_2 and 5% O_2. Embryos were fixed at room temperature in 4% paraformaldehyde for 30 minutes, and then washed several times in 0.1% Tween-20 in PBS. Embryos were permeabilized in 1% Tween-20 in PBS at 4 °C for 4 days on a rotating shaker and then blocked in 10% FBS and 0.2% Tween-20 in PBS at room temperature for 1 hour. Embryos were incubated in a 1:100 dilution of primary antibody in blocking buffer at 4°C overnight on a rotating shaker and washed several times in 0.1% Tween-20 in PBS at room temperature. Embryos were incubated in a 1:500 dilution of secondary antibody anti-rabbit Alexa Fluor 555 (Invitrogen) in blocking buffer at room temperature for 1 hour while protected from light. They were then washed several times in 0.1% Tween-20 in PBS and mounted in ProLong Diamond with DAPI (Invitrogen) on a glass slide, covered with a glass coverslip and left at room temperature to cure overnight. Images were taken using a LSM780 confocal microscope (Zeiss).

Glucose Consumption and Lactate Production Rates

Cellular glucose consumption and lactate export rates were measured using a Nova Biomedical BioProfile Basic Analyzer. Briefly, cells were seeded in triplicates in 6-well plates at usual passing density. Ninety-six hours post-seeding, when the colonies were subconfluent, cells were washed with PBS, and 1ml fresh medium was added to each well, including an empty well without any cells as a blank control. After 24-hour incubation, culture medium was collected and then analyzed by the Nova BioProfile analyzer. Cell numbers were determined both before and after the 24-hour incubation period using a Coulter particle analyzer and used to normalize the calculated rates. Among different figures, the same cell line might show different values in glucose and lactate readings, which was due to the difference in cell numbers between different experiments. Since plating density of cells can impact metabolism, we always ensured that different treatment groups or cell lines within a given experiment had similar cell counts when glucose and lactate measurements were taken. We accomplished this by plating hESCs at different densities and measuring the media glucose and lactate amounts in the ones with similar cell counts.

Oxygen Consumption Rates

For comparing oxygen consumption rates in feeder-supported hESCs, cells were treated with Accutase (Invitrogen) for 5 minutes after PBS wash, passed through a 40-μm cell strainer (BD), and cell count was obtained. Four million cells were spun down at 300g for 5 minutes, resuspended in 250 μl culture medium, and transferred to an anaerobic chamber of 250 μl volume. The anaerobic chamber was maintained at 37 °C by a water circulating system (DC10, Thermo), and fitted with a fiber optic oxygen sensor (Model 110, INSTECH). Oxygen concentration was sensed by the quenching of fluorescence of

an indicator dye trapped in a matrix at the tip of the probe, and was calibrated with 15 mM sodium hydrosulfite (Sigma) and cell culture media, corresponding to 0% and 20.9% oxygen respectively.

Extracellular Acidification and Oxygen Consumption Rates

For comparing extracellular acidification and oxygen consumption rates in feeder-free primed hESCs, with AZD3965 or DMSO treatment, cells were seeded onto an XF24 Cell Culture Microplate (Seahorse Bioscience) at 2 - 7.5 × 10^4 cells/well with the 10 μM ROCK inhibitor Y-27632 (Calbiochem) and incubated at 37°C overnight. Extracellular acidification and oxygen consumption rates were measured by using an XF24 Extracellular Flux Analyzer (Seahorse Bioscience) in unbuffered DMEM assay medium supplemented with 1mM pyruvate and 25mM glucose after 45 to 60-minute equilibration, and were normalized to protein concentration using the Protein Assay reagent (Bio-Rad).

Mass Spectrometry-based Metabolomics Analysis

Cells were incubated in medium containing 3.151 g/l 1,2-^{13}C-glucose for 24 hours. The following day, cells were rinsed with cold 150 mM ammonium acetate (NH_4AcO). Cells were carefully scraped off in 800 μl of 50% ice cold methanol. An internal standard of 12.5 μM norvaline was added to the cell suspension, followed by 400 μl of cold chloroform. After vortexing for 15 min, the aqueous layer was transferred to a glass vial and the metabolites were dried under vacuum. Metabolites were resuspended in 100 μl 70% acetonitrile (ACN) and 5 μl of this solution was used for the mass spectrometer-based analysis. The analysis was performed on a Q Exactive (Thermo Scientific) in polarity-switching mode with positive voltage 3.0 kV and negative voltage 2.25 kV. The mass spectrometer was coupled to an UltiMate 3000RSLC (Thermo Scientific) UHPLC

system. Mobile phase A was 5 mM NH_4AcO, pH 9.9, B was ACN, and the separation achieved on a Luna 3mm NH_2 100A (150 x 2.0 mm) (Phenomenex) column. The flow was 300 µl/min, and the gradient ran from 15% A to 95% A in 18 min, followed by an isocratic step for 9 minutes and re-equilibration for 7 minutes. Metabolites were detected and quantified as area under the curve (AUC) based on retention time and accurate mass (≤ 3 ppm) using the TraceFinder 3.1 (Thermo Scientific) software. Relative amounts of metabolites between various conditions, as well as percentage of labeling were calculated and corrected for naturally occurring ^{13}C abundance (Yuan et al., 2008; Moseley, 2010). For the heatmap depiction of the relative amounts of glycolytic intermediates, Z scores were calculated by subtracting the mean value across all samples, then dividing over standard deviation (SD). When feeder-supported and feeder-free primed hESCs were compared, a plate of irradiated MEFs without hESCs was also labeled with 1,2-^{13}C-glucose, and traced the incorporation of ^{13}C into downstream glucose metabolites using LC-MS, to control for the presence of feeder cells in the FS conditions (Figure S4A-D, and Fan et al., 2014; Yuan et al., 2008).

Immunoblot Assays

For preparing whole cell lysates, cells were lysed in M-PER Mammalian Protein Extraction Reagent (Thermo) with 20 mM NaF, 1 mM Na_3VO_4, 4 µg/ml aprotinin, 4 µg/ml leupeptin, 4 µg/ml pepstatin, and 1 mM DTT. Nuclear and cytoplasmic fractions were prepared using the following protocol: Buffer A, containing 10 mM HEPES (pH 7.9), 10 mM KCl, 0.1 mM EDTA, 0.4% NP40, 20 mM NaF, 1 mM Na_3VO_4, 4 µg/ml aprotinin, 4 µg/ml leupeptin, 4 µg/ml pepstatin, and 1 mM DTT, was used to extract cytoplasmic proteins; Nuclear pellet was resuspended in Buffer B, which contains 20 mM

HEPES (pH 7.9), 400 mM NaCl, 1mM EDTA, 10% glycerol, 20 mM NaF, 1 mM Na_3VO_4, 4 μg/ml aprotinin, 4 μg/ml leupeptin, 4 μg/ml pepstatin, and 1 mM DTT, and placed on vortex at 4 °C for 2 hours to extract nuclear proteins. Western blot analysis was carried out according to standard methods. Protein concentrations of cell extracts were determined by using the Protein Assay reagent (Bio-Rad). The following commercial antibodies were used as probes: C-MYC, N-MYC, OCT4A, TBP (Cell Signaling), β-Tubulin (Sigma), MCT1, and GAPDH (Abcam).

RNA-Seq

Feeder-supported UCLA1 primed and naive hESCs were cultured in a 6-well dish. Primed hESCs were harvested with 1mg/ml Collagenase IV (Life Technologies) for 8min at 37 °C, or until the edges of colonies lifted off slightly. Colonies were collected in hESM followed by sequential sedimentation steps to deplete feeder cells. Colonies were then washed once in PBS and collected in 1ml Trizol (Invitrogen). Naive hESCs were feeder depleted by treating the cells with Accutase and passing the cells through a 40-μm mesh. Under these conditions feeder cells do not separate into single cells and therefore do not pass through the filter. Cells were collected in 1 ml Trizol after a PBS wash. Total RNA was isolated by phenol chloroform extraction and purified by RNeasy Mini Kit (Qiagen). The TruSeq Stranded mRNA Library Prep Kit (Illumina) was used to prepare mRNA libraries following manufacturer's instructions. The libraries were run on 2% SeaPlaque Agarose gel (Lonza) to remove primer contaminants, and purified using MinElute Gel Extraction Kit (Qiagen). Final library amounts were quantified by Qubit dsDNA HS Assay (Invitrogen) and sequenced on Illumina HiSeq 2500 instrument at the UCLA High-Throughput Sequencing Facility. Reads were mapped to hg19 assembly of

the human genome using the TopHat read-mapping algorithm (Trapnell et al., 2009), and gene expression levels were calculated as RPKM values (Mortazavi et al., 2008).

Microarray and Enrichment Analysis

Total RNA was isolated by using the Absolutely RNA kit (Stratagene) and reverse-transcribed with the SuperScript III First-Strand Synthesis System (Invitrogen) with oligo dT primers. Whole-genome expression analysis was performed with the HG-U133 plus 2 array (Affymetrix) at the UCLA Clinical Microarray Core.

Gene Set Enrichment Analysis (Subramanian et al., 2005) was performed using the Molecular Signatures Database (MSigDB) C2 collection (version 5.0) of canonical signaling pathways, cellular processes, chemical and genetic perturbations, and human disease states. For GSEA on primed hESCs with AZD3965 or DMSO treatment, readings of probe sets were first RMA normalized, and then collapsed according to the probes with maximum expression values into gene symbols, which were then ranked according to the log10 p value from paired t-test between AZD3965 and DMSO groups in three hESC lines: H1, H9, and HSF1. Pre-ranked GSEA was also conducted on naive and primed UCLA1 hESCs.

For human preimplantation datasets, each data was analyzed separately. The mRNA microarray dataset by Vassena et al., 2011(GEO accession: GSE29397), was processed using Bioconductor package in R, normalized using the RMA method, and then imported to GSEA. The single-cell RNA-Seq dataset by Yan et al., 2013 (GEO accession: GSE36552) contained the gene expression levels presented as RPKM values, based on which the log fold changes (base 2) were calculated and ranked to generate an ordered gene list for Pre-ranked GSEA.

For the enriched MYC-regulated gene sets identified by GSEA, MENSSEN_MYC_TARGETS was first reported by Menssen et al. (Menssen and Hermeking, 2002), SCHLOSSER_MYC_TARGETS_REPRESSED_BY_SERUM was based on published data by Schlosser et al. (Schlosser et al., 2005), and DANG_MYC_TARGETS_UP was reported by Zeller et al. (Zeller et al., 2003). Details about each gene set can also be found at http://software.broadinstitute.org/gsea/msigdb/. A web-based application GOrilla (Eden et al., 2009) was used to identify enriched Gene Ontology (Ashburner et al., 2000) terms in a ranked list of all genes according to the differential expression in AZD3965 versus DMSO-treated H1, H9, and HSF1 hESCs.

Cell Proliferation

Cells were seeded in triplicates in 6-well plates, and cell counts were obtained using a Coulter particle analyzer 5 days after seeding.

SUPPLEMENTAL REFERENCES

Ashburner, M., Ball, C.A., Blake, J.A., Botstein, D., Butler, H., Cherry, J.M., Davis, A.P., Dolinski, K., Dwight, S.S., Eppig, J.T., et al. (2000). Gene Ontology: tool for the unification of biology. Nat. Genet. *25*, 25–29.

Eden, E., Navon, R., Steinfeld, I., Lipson, D., and Yakhini, Z. (2009). GOrilla: a tool for discovery and visualization of enriched GO terms in ranked gene lists. BMC Bioinformatics *10*, 48.

Fan, J., Ye, J., Kamphorst, J.J., Shlomi, T., Thompson, C.B., and Rabinowitz, J.D. (2014). Quantitative flux analysis reveals folate-dependent NADPH production. Nature *510*, 298–302.

Menssen, A., and Hermeking, H. (2002). Characterization of the c-MYC-regulated transcriptome by SAGE: Identification and analysis of c-MYC target genes. Proc. Natl. Acad. Sci. *99*, 6274–6279.

Mortazavi, A., Williams, B.A., McCue, K., Schaeffer, L., and Wold, B. (2008). Mapping and quantifying mammalian transcriptomes by RNA-Seq. Nat. Methods *5*, 621–628.

Moseley, H.N. (2010). Correcting for the effects of natural abundance in stable isotope resolved metabolomics experiments involving ultra-high resolution mass spectrometry. BMC Bioinformatics *11*, 139.

Schlosser, I., Hölzel, M., Hoffmann, R., Burtscher, H., Kohlhuber, F., Schuhmacher, M., Chapman, R., Weidle, U.H., and Eick, D. (2005). Dissection of transcriptional programmes in response to serum and c-Myc in a human B-cell line. Oncogene *24*, 520–524.

Subramanian, A., Tamayo, P., Mootha, V.K., Mukherjee, S., Ebert, B.L., Gillette, M.A., Paulovich, A., Pomeroy, S.L., Golub, T.R., Lander, E.S., et al. (2005). Gene set enrichment analysis: A knowledge-based approach for interpreting genome-wide expression profiles. Proc. Natl. Acad. Sci. *102*, 15545–15550.

Takashima, Y., Guo, G., Loos, R., Nichols, J., Ficz, G., Krueger, F., Oxley, D., Santos, F., Clarke, J., Mansfield, W., et al. (2014). Resetting Transcription Factor Control Circuitry toward Ground-State Pluripotency in Human. Cell *158*, 1254–1269.

Theunissen, T.W., Powell, B.E., Wang, H., Mitalipova, M., Faddah, D.A., Reddy, J., Fan, Z.P., Maetzel, D., Ganz, K., Shi, L., et al. (2014). Systematic Identification of Culture Conditions for Induction and Maintenance of Naive Human Pluripotency. Cell Stem Cell *15*, 471–487.

Trapnell, C., Pachter, L., and Salzberg, S.L. (2009). TopHat: discovering splice junctions with RNA-Seq. Bioinformatics *25*, 1105–1111.

Vassena, R., Boué, S., González-Roca, E., Aran, B., Auer, H., Veiga, A., and Belmonte, J.C.I. (2011). Waves of early transcriptional activation and pluripotency program initiation during human preimplantation development. Development *138*, 3699–3709.

Yan, L., Yang, M., Guo, H., Yang, L., Wu, J., Li, R., Liu, P., Lian, Y., Zheng, X., Yan, J., et al. (2013). Single-cell RNA-Seq profiling of human preimplantation embryos and embryonic stem cells. Nat. Struct. Mol. Biol. *20*, 1131–1139.

Yuan, J., Bennett, B.D., and Rabinowitz, J.D. (2008). Kinetic flux profiling for quantitation of cellular metabolic fluxes. Nat. Protoc. *3*, 1328–1340.

Zeller, K.I., Jegga, A.G., Aronow, B.J., O'Donnell, K.A., and Dang, C.V. (2003). An integrated database of genes responsive to the Myc oncogenic transcription factor: identification of direct genomic targets. Genome Biol. *4*, R69.